EC
Journals.ASM.org

The *Giardia* Median Body Protein Is a Ventral Disc Protein That Is Critical for Maintaining a Domed Disc Conformation during Attachment

David J. Woessner and Scott C. Dawson

Department of Microbiology, University of California, Davis, Davis, California, USA

Giardia **has unique microtubule structures, including the ventral disc, the primary organelle of attachment to the host, and the median body, a structure of undefined function. During attachment, the ventral disc has a domed conformation and enables *Giardia* to attach to the host intestinal epithelia within seconds. The mechanism of attachment via the ventral disc and the overall structure, function, and assembly of the ventral disc are not well understood. Our recent proteomic analysis of the ventral disc indicated that the median body protein (MBP), previously reported to localize exclusively to the median body, was primarily localized to the ventral disc. Using high-resolution light and electron microscopy, we confirm that the median body protein localizes primarily to the overlap zone of the ventral disc. The MBP also occasionally localized to the median body during prophase. To define the contribution of MBP to the ventral disc structure, we depleted MBP using an anti-MBP morpholino. We found that the ventral disc was no longer able to form properly and that the disc structure often had an aberrant nondomed or flattened horseshoe conformation. The ability of attached anti-MBP morpholino-treated trophozoites to withstand shear forces and normal forces was significantly decreased. Most notably, the plasma membrane contacts with the surface, including those of the bare area, were defective after the anti-MBP knockdown. To our knowledge, this is the first ventral disc protein whose depletion directly alters ventral disc structure, confirming that the domed ventral disc conformation is important for robust attachment.**

Giardia intestinalis is a parasitic protist that causes giardiasis, a diarrheal disease infecting millions worldwide. Infection with *Giardia* is exceedingly common in developing countries due to a lack of adequate water treatment (35, 37). *Giardia*'s two-stage life cycle consists of an infectious cyst form that is found in the environment (1, 13) as well as a trophozoite form that colonizes the intestinal tract of the host. Triggered by their passage through the acidity of the stomach, *Giardia* cysts excyst in the small intestine of the host and the motile trophozoites attach to the intestinal epithelium via the ventral disc (1). The lack of research into basic *Giardia* biology and a lack of effective and affordable methods of treatment have led the World Health Organization (WHO) to name giardiasis a neglected disease (35). As *Giardia* continues to become more resistant to the drug metronidazole, it becomes increasingly important to discover new ways to treat this common parasitic infection (3, 28, 39).

The ability of trophozoites to position themselves in the small intestine, attach to the epithelium, and thereby colonize the host is contingent upon *Giardia*'s complex microtubule cytoskeleton. The interphase microtubule cytoskeleton of *Giardia* is comprised of the ventral disc, the median body, four pairs of flagella, and the funis (10). *Giardia*'s attachment to its host is mediated by the ventral disc (13). The ventral disc is a complex microtubule-based structure (~150 to 400 nm thick) composed of a right-handed spiral sheet of microtubules (MTs) and associated structures of unknown function. The ventral disc forms a complete spiral, which results in a small region where the upper and lower portions of the disc overlap, the overlap zone. Extending dorsally from the MTs are trilaminar microribbons, connected by cross bridges that attach to ventral disc MTs along the entire length of the spiral. Surrounding the ventral disc is another ordered structure known as the lateral crest (16). Attachment is a rapid stepwise process in which a seal with the surface is formed by the lateral crest (25) and the ventral disc adopts a dome-shaped conformation (23). This seal formed by the lateral crest may permit a suction-based mechanism of attachment. It remains unclear whether conformational changes of the ventral disc directly create forces for attachment or if disc conformational dynamics maintain attachment forces that are generated by some other mechanism (20, 25).

The other conspicuous microtubule structure in *Giardia*, the median body, is an enigmatic structure of unknown function that often forms the "crooked smile" in *Giardia* images (10). Median body microtubules are dynamic (12) and are thought to be somewhat disordered. The median body is hypothesized to have a role in ventral disc biogenesis, serving perhaps as a reservoir of polymerized MTs (14). Several microtubule-associated proteins have been shown to localize to the median body, including kinesin-13 and EB1 (12). Overexpression of a dominant negative form of kinesin-13 results in decreases in median body volume (12), suggesting that this depolymerizing kinesin motor regulates median body microtubule dynamics.

The functions of the ventral disc structural elements (or the proteins that comprise them) in generating or maintaining attachment are not well understood. We have recently identified over 18 new ventral disc and lateral crest structural proteins, more than

Received 11 October 2011 **Accepted** 4 January 2012
Published ahead of print 13 January 2012
Address correspondence to Scott C. Dawson, scdawson@ucdavis.edu.
Supplemental material for this article may be found at http://ec.asm.org/.

doi:10.1128/EC.05262-11

doubling the number of known ventral disc components (19). One abundant disc-associated protein (DAP) identified in our previous proteomic analysis of the ventral disc (19) was the so-called median body protein (MBP; DAP16343). MBP was first identified through an antibody screen and reported to localize exclusively to the median body by immunolocalization (29). MBP has no significant similarity to any known microtubule-associated protein and appears to be novel to *Giardia* (29, 30).

In this study, we confirmed the ventral disc localization of MBP using both green fluorescent protein (GFP)- and epitope-tagging approaches. To understand the function of this abundant disc-associated protein, we used a morpholino-based knockdown approach to disrupt translation of MBP. We observed that introduction of an anti-MBP morpholino resulted in significant defects in attachment by both biophysical assays and microscopic examination of surface contacts using total internal reflection fluorescence microscopy (TIRFM) (25). A significant proportion of anti-MBP-treated trophozoites had open disc or horseshoe-shaped disc conformations. Using three-dimensional (3D) microscopy, we show that trophozoites with the open disc have a flat, not a domed, conformation upon attachment. We contend, therefore, that a dome-shaped disc conformation is critical for robust attachment.

MATERIALS AND METHODS

Strains and culture conditions. *Giardia intestinalis* strain WBC6 (ATCC 50803) trophozoites were maintained at 37°C in modified TYI-S-33 medium with bovine bile (26) in 16-ml screw-cap tubes (Fisher Scientific). For live imaging experiments, trophozoites were also grown on coverslips placed in 8-well dishes in a sealed chamber (PlasLabs) and gassed with 100% N_2 to maintain a low-oxygen atmosphere. This chamber was incubated at 37°C prior to live cell imaging as previously described (11).

Construction of the C-terminal GFP-tagged median body protein strain and the strain with integrated MBP::3HA. The MBP::GFP strain was constructed by PCR amplification of the MBP gene from *Giardia* genomic DNA using the following primers: primer MBPF (5′-GGCGCG CCATGTCCGAGGCTATGGTTTTCAGCAAGATCG-3′) and primer MBPR (5′-ACCGGTAGCCCTGCCCCTGCCCCTGCCGCCGCGAACT TACCACTTCGGCCC-3′). This amplification yielded the MBP gene flanked by 5′ AscI and 3′ AgeI restriction sites, and the amplicon was subsequently cloned into the pTetGFPC.pac episomal plasmid (12). The MBP::GFP construct was transformed into *Giardia intestinalis* strain WBC6 by electroporation using 10 μg of plasmid DNA and a GenePulserXL apparatus (Bio-Rad) as previously described (12) with the following modifications: 375 V, 1,000 μF, and 25 Ω. Episomal MBP::GFP constructs were maintained in transformants using antibiotic selection (50 μg/ml puromycin) (9).

The C-terminal median body protein fragment was cloned in frame to a triple-hemagglutinin (3HA) epitope tag and then ligated into a pJET vector containing a neomycin resistance gene (18). This vector was linearized with StuI, and trophozoites were transformed by electroporation as described previously (18). Transformed trophozoites were selected and maintained with neomycin G418 at 400 μg/ml.

Immunofluorescence microscopy and image data analysis. Immunostaining of the GFP-tagged MBP and HA-tagged MBP strains was performed as previously described (34). Briefly, trophozoites were incubated in HEPES-buffered saline (HBS) for 30 min. Cells were then fixed in 1% paraformaldehyde for 30 min at 37°C. After fixation, cells were pelleted by centrifugation at 900 × *g* for 5 min, washed once in 1 ml PEM buffer {100 mM PIPES [piperazine-*N*,*N*′-bis(2-ethanesulfonic acid)], 1 mM EGTA, 0.1 mM $MgSO_4$}, and resuspended in 200 μl PEM. These cells were then settled onto poly-L-lysine-coated coverslips for 15 min. Cell-coated coverslips were then washed three times with PEM. Cells were next permeabilized with 0.1% Triton X-100 for 10 min, washed three times in PEM, and incubated in PEM with 1% bovine serum albumin, 0.1% sodium azide, 100 mM lysine, and 0.5% cold-water fish skin gelatin (Sigma, St. Louis, MO) (PEMBALG) for 30 min. The coverslips were incubated with TAT1 (1:200), anti-HA (1:1000), or anti-β-giardin (1:200) antibody overnight. The following day, coverslips were washed three times in PEMBALG. The coverslips were then incubated with Alexa Fluor 594 goat anti-mouse IgG secondary antibody (1:200; Invitrogen) for 2 h, washed three times in PEMBALG and PEM, and counterstained with 4′,6-diamidino-2-phenylindole (DAPI).

To confirm localization, Metamorph image acquisition software (MDS Technologies) was used to collect 3D images using a Leica DMI 6000 wide-field inverted fluorescence microscope with a PlanApo ×100, 1.40-numerical-aperture (NA) oil-immersion objective. Serial sections of DAP::GFP strains were acquired at 0.2-μm intervals and deconvolved using Huygens Professional deconvolution software (Scientific Volume Imaging). Two-dimensional maximum-intensity projections were created from the 3D data sets for presentation purposes.

Live cell imaging of attachment in the MBP-knockdown cells using TIRFM and differential interference contrast (DIC). We used TIRFM (2) to determine if trophozoite and disc surface contacts were aberrant after morpholino knockdown of the MBP. Trophozoites were resuspended in 1× HBS and incubated on ice for 10 min. To stain cell membranes, trophozoites were incubated for an additional 5 min on ice with CellMask Orange (final concentration, 2 μg/ml; Invitrogen). Stained cells were concentrated by centrifugation (900 × *g* for 5 min) and resuspended in 500 μl of warmed (37°C) 1× HBS prior to imaging. A simple imaging chamber was created as previously described (25). Live cell imaging was performed in a microscope-stage incubator (OkoLab) at a temperature of 35 to 37°C using 488- and 561-nm lasers with 10- to 100-ms exposures; no charge-coupled-device (CCD) gain was used. Images were collected with a QuantEM 512 SC electron-multiplying CCD camera (Photometrics) on a 3i Marianas inverted spinning-disc confocal microscope system. Slidebook software (Intelligent Imaging Innovations) was used for minor image processing, such as cropping and two-dimensional intensity plots.

Negative staining and immunolabeling of isolated discs from DAP::GFP fusions. To determine the localization of the MBP in the ventral disc structure, detergent-extracted cytoskeletons from the MBP::GFP strain were isolated (19) and immunolabeled for negative staining of the MBP as previously described (40). Cytoskeletons were placed in a blocking buffer of 3% nonfat dry milk in PHEM buffer (60 mM PIPES, 25 mM HEPES, 10 mM EGTA, 2 mM $MgCl_2$) for 1 h. The MBP::GFP cytoskeletons were then labeled with an anti-GFP antibody in blocking buffer for 1.5 h and rinsed three times for 15 min each in PHEM. Samples were incubated with 5 nm goat anti-rabbit $F(ab')_2$ IgG antibody (BB International) in blocking buffer for 1 h and rinsed three times for 15 min each in PHEM. For negative controls, only the secondary antibody was used.

For negative staining of the MBP::GFP fusion strain, 300-mesh copper grids (Electron Microscopy Sciences) were Formvar coated, carbon coated, and then glow discharged to make them more hydrophilic. A 5-μl droplet of the MBP::GFP disc preparation was placed on the grid, blotted, and then negative stained with a 5-μl droplet of 2% aqueous uranyl acetate (Ted Pella) and again blotted. Grids were imaged on an Advanced Microscopy Techniques digital camera in a CM100 (FEI) transmission electron microscope operating at 80 kV.

Morpholino-based knockdown of MBP. Morpholinos were designed to target the first 24 bases of the MBP-encoding gene and 1 base upstream of the 5′ end. The resulting anti-MBP morpholino sequence was 5′-GCT GAAAACCATAGCCTCGGACATT-3′. A mispair morpholino with the sequence 5′-GGTGAAAAGCATAGGCTCCGAGATT-3′ was used as a control for off-target effects. Prior to MBP morpholino knockdown, trophozoites of either the wild-type strain WBC6, the lateral crest DAP17096::GFP-tagged strain (19), or the integrated MBP::3HA strain were grown to confluence. Cells were washed with 12 ml of fresh medium, quickly suspended again in 12 ml of medium, and then chilled on ice for 20 min. The detached trophozoites were then centrifuged at 900 × *g* for 5

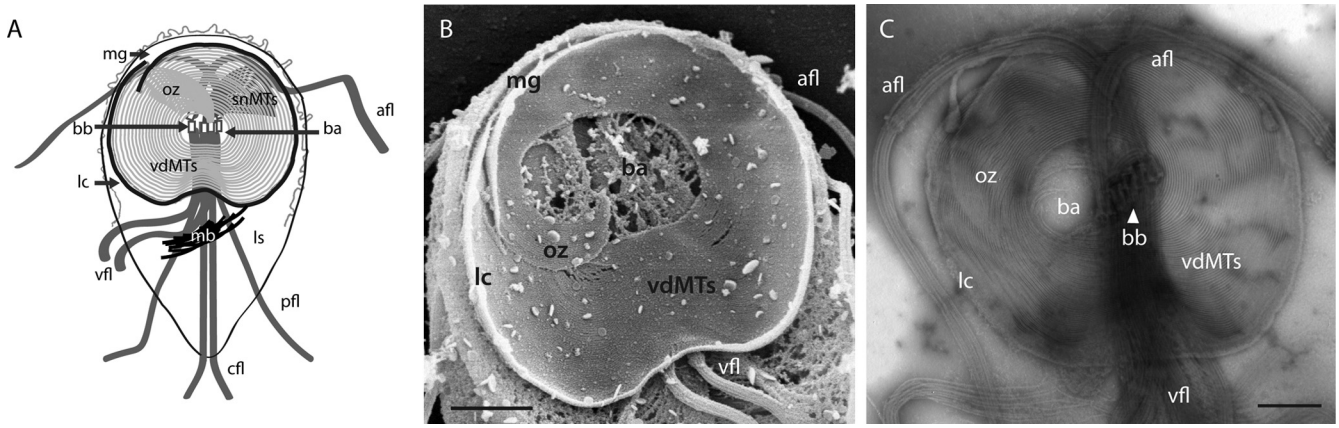

FIG 1 Overall architecture of the ventral disc highlighting the overlap zone. (A) A schematic view of the *Giardia* cytoskeleton shows the median body (mb), the ventral disc MT (vdMT) and supernumerary MT (snMT) spiral arrays, the overlap zone (oz) of the ventral disc MTs, the lateral crest (lc), the basal bodies (bb), and the four flagellar pairs (ventral flagella [vfl], caudal flagella [cfl], posteriolateral flagella [pfl], and anterior flagella [afl]). mg, marginal groove; ba, bare area. (B) A scanning electron micrograph of the detergent-extracted cytoskeleton highlights the overlap zone, the cellular regions underlying the bare area, the marginal groove, and the lateral crest as viewed from the ventral side. (C) Negative staining of the detergent-extracted cytoskeleton shows the cytological positions of the anterior and ventral flagella relative to the ventral disc as seen from the dorsal side and highlights hallmark features, such as the regular and evenly spaced microtubules of the ventral disc overlapping one-quarter turn in the overlap zone.

min at 4°C. The resulting pellet was resuspended in 0.27 ml of fresh medium. This was added to a 0.4-mm electroporation cuvette along with morpholino at a final concentration of 100 μM. The cuvette was chilled on ice for 5 min, and electroporation was performed as described above, with the only modification being the use of 350 V instead of 375 V. These transformed cells were then incubated at 37°C for 48 h. Following electroporation of the MBP-specific morpholino oligonucleotides or controls, cell morphology and attachment were assessed in both live and fixed trophozoites.

Quantification of anti-MBP morpholino knockdown in the MBP::3HA strain. To determine the extent of MBP knockdown, Western blotting was used to assay the HA-tagged MBP levels in extracts from the integrated 3HA-tagged MBP strain compared to those from the WBC6 strain. Forty-eight hours after electroporation of the anti-MBP or missense oligonucleotide, trophozoites were placed on ice for 15 min to promoted detachment. Detached trophozoites were then centrifuged, and the resulting pellet was washed in 1× HBS containing Halt protease inhibitor cocktail (ThermoScientific). Cells were pelleted again and resuspended in 1× Laemmli buffer, and the suspension was then boiled for 5 min. This cell extract was loaded onto a 12% SDS-polyacrylamide gel, separated by electrophoresis, and transferred to Immobilon-FL polyvinylidene difluoride membranes. Membranes were blocked, and the MBP::3HA protein was detected using a 1:10,000 dilution of anti-HA antibody (mouse monoclonal; H9658; Sigma) and a horseradish peroxidase-conjugated secondary antibody (Bio-Rad) at a 1:5,000 dilution. The blot was also probed with antitubulin antibody TAT1 at 1:2,500 to normalize loading. The degree of MBP knockdown was quantified using an Alpha Innotech Gel imaging and documentation system (Cell Biosciences).

Quantification of attachment shear forces using a laminar-flow assay. The effect of shear forces on live trophozoites attached to a glass substrate was imaged using a syringe pump to create laminar flow with a temperature-controlled Harvard Apparatus RC-31 parallel-plate flow cell chamber (Warner Instruments) mounted onto an inverted Nikon Eclipse TS100 microscope with a 10×, 0.25-NA ADL objective and a Retiga 2000R CCD (Qimaging) as previously described (20, 25). Shear-force experiments were performed on trophozoites 48 h after the introduction of the MBP morpholino. A preassay image was taken (time zero). Cells were then challenged with a 3-ml/min laminar-flow rate (20) for 3 min as images were captured at 10-s intervals via phase-contrast. To quantify the fraction of cells that maintained attachment over a range of shear forces, cell counting was performed manually or using Metamorph image acquisition software (MDS Technologies). The proportion of attached morpholino-treated cells was normalized to the proportion of wild-type water-electroporated control trophozoites.

Assessing normal forces of attachment using a centrifuge assay. Defects in the normal forces of attachment in trophozoites were assayed at the population level using a physical attachment assay (21). Forty-eight hours after the electroporation of the anti-MBP morpholino, trophozoites were pelleted on ice. Trophozoites were resuspended in 10 ml of chilled medium, and then 3 ml was transferred to custom sample holders capped with thick, circular glass slides. The cells were incubated at 37°C for 1 h in a micro-oxic chamber to allow attachment to the glass slides (11). Sample holders were centrifuged at 37°C in a hanging-bucket centrifuge (Sorvall RC5C HB4 rotor 07) at 10,000 rpm (2.1 nN normal force). Noncentrifuged controls were prepared in the same manner and incubated at 37°C. The glass slides were removed from the chamber immediately after centrifugation. Five fields (~5,000 cells) were imaged and counted using phase-contrast. The proportion of trophozoites maintaining attachment was normalized to the noncentrifuged control.

Analysis of MBP turnover using fluorescence recovery after photobleaching (FRAP). We used laser fluorescence photobleaching of specific regions of the ventral disc to measure the movement and steady-state turnover of the MBP, a technique that has been used extensively in other organisms (36). MBP::GFP-expressing trophozoites were embedded in 1% low-melt agarose and imaged using an Olympus FV1000 scanning laser confocal microscope equipped with a four-channel photomultiplier tube. To photobleach a specific region of MBP localization, we used 95% 405-nm laser power for 2 s. The 488-nm laser was used to acquire the prebleach image of the cell. Fluorescence recovery in the MBP::GFP strain was analyzed by imaging once every minute for up to 10 min using the 488-nm low-power laser excitation (see Fig. S2 in the supplemental material for supporting information).

Nucleotide sequence accession numbers. MBP has been placed in GenBank under accession number Q08014 and the GiardiaDB under accession number GL50803_16343.

RESULTS

The median body protein localizes primarily to the ventral disc. To gain insight into the function of the MBP, we constructed a C-terminal GFP-tagged MBP and transformed this MBP::GFP fusion construct into *Giardia* trophozoites. The ventral disc is com-

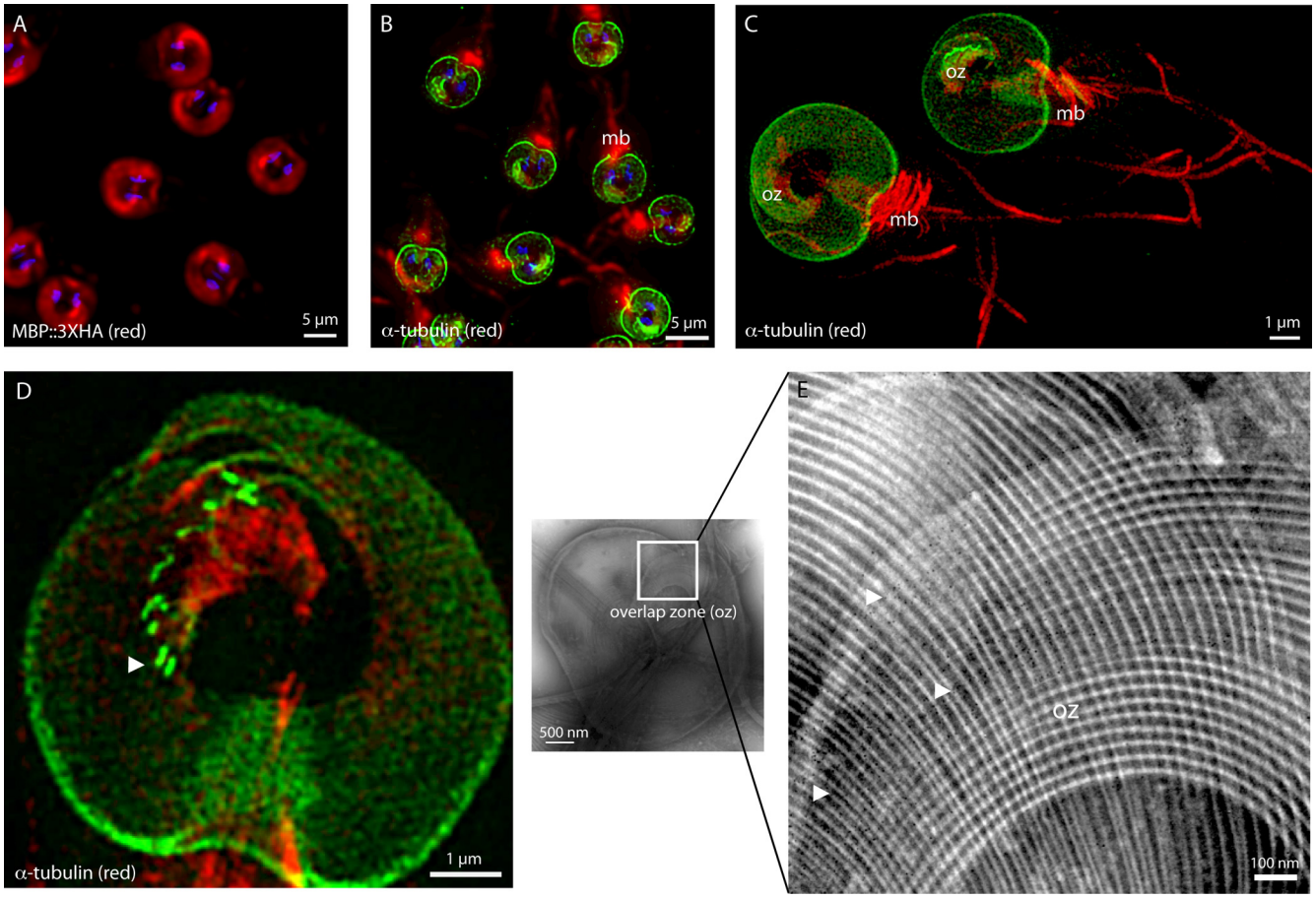

FIG 2 MBP localizes primarily to the ventral disc. Ventral disc localization of MBP visualized in the MBP::3HA and MBP::GFP strains using conventional and superresolution light microscopy or electron microscopy with anti-GFP immunogold labeling with negative staining. (A) Localization of 3HA epitope-tagged MBP (red) to the entire ventral disc in all cells with occasional localization to the median body. (B) Similar localization of GFP-tagged MBP (green) to the entire disc with occasional localization to median body microtubules (mb) in cells immunostained with anti-α-tubulin antibody (red). Nuclei are stained with DAPI (blue). (C and D) Super-resolution structured illumination imaging of the MBP::GFP strain immunostained with anti-α-tubulin (green, GFP; red, α-tubulin) shows detailed localization of MBP to the ventral disc spiral, with some concentration at the overlap zone (oz) of the ventral disc microtubule spiral (C) and the microtubule plus ends of the spiral (D, arrowhead). (E) Negative staining shows a high concentration of 5-nm nanogold particles localized to the overlap zone (arrows).

posed of a regularly spaced spiral MT array with associated structures (10) surrounded by a fibrillar lateral crest and overlaps one and one-quarter turns around a central bare area ventral to the flagellar basal bodies (Fig. 1). Using deconvolution epifluorescence microscopy, we observed median body protein throughout the ventral disc in 100% of cells concentrated most prominently at the disc edges, the overlap zone (Fig. 1), and the plus ends of the MT spiral array, as seen using superresolution light microscopy (Fig. 2). The median body protein also localizes close to the microtubules but not to the microribbons or cross bridges, as visualized using negative staining of the MBP::GFP strain with an anti-GFP primary antibody coupled with 10-nm immunogold (Fig. 2). To confirm the localization of MBP to the ventral disc, we integrated a copy of MBP::3HA into the wild-type *Giardia* genome under the control of its native promoter as previously described (18). The epitope-tagged MBP::3HA also localized primarily to the ventral disc and only infrequently to the median body (Fig. 2).

In contrast to prior studies (29), the median body localization of the MBP was observed in only ~20% of trophozoites; these were primarily in prophase, as evidenced by chromosome condensation in both nuclei (34). Using FRAP, we also observed that MBP::GFP localization does not recover either to the ventral disc or to the median body following photobleaching (see Fig. S1 in the supplemental material for supporting information).

Morpholino knockdown of MBP results in open discs and mispositioning and discontinuity of the lateral crest. To assess the function of MBP in the ventral disc, we used a morpholino knockdown (6) to block translation of the median body protein. We observed over 55% knockdown of MBP by Western blotting 48 h following the electroporation of an anti-MBP morpholino in the strain with integrated MBP::3HA compared to the nonelectroporated controls (see Fig. S1 in the supplemental material for supporting information). Using fluorescently tagged morpholinos, the percentage of trophozoites that retain an electroporated morpholino in *Giardia* has been quantified to be over 95% of cells (6), with a 60 to 80% knockdown generally observed for several cytoskeletal proteins (6, 25, 32).

To characterize the ventral disc structure and attachment phenotypes arising from the median body protein knockdown, we electroporated the anti-MBP morpholino into a δ-giardin::GFP

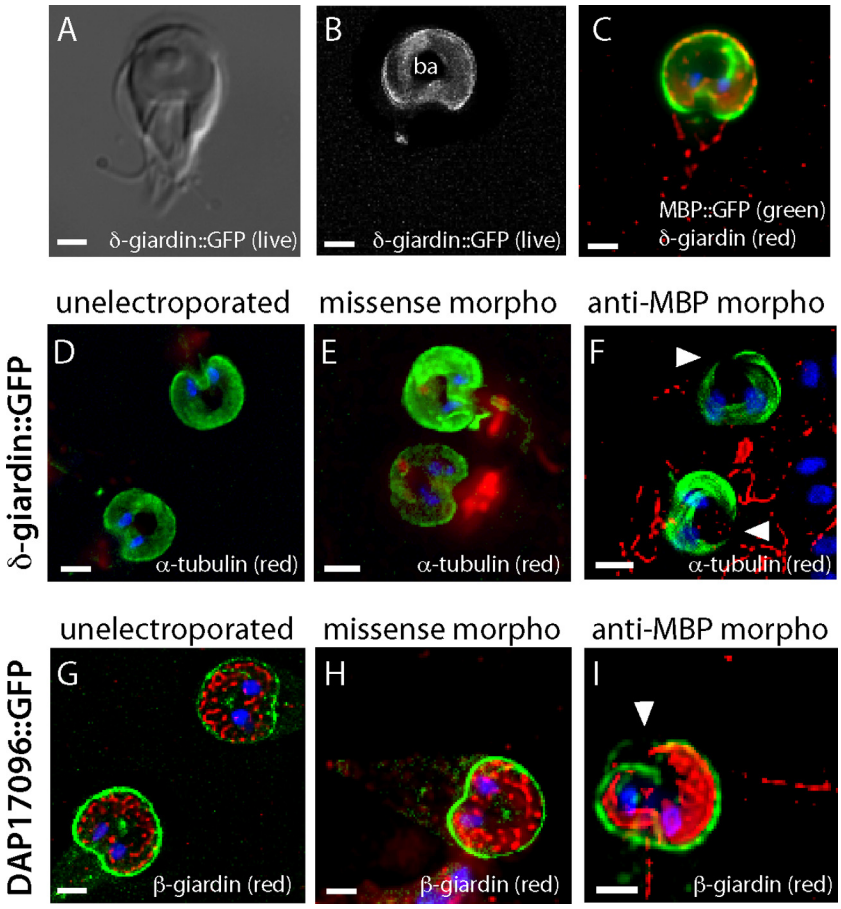

FIG 3 The morpholino knockdown of MBP results in an open or horseshoe-shaped disc conformation and a discontinuous lateral crest. (A and B) The ventral disc (vd) localization of δ-giardin and the viability of ventral disc GFP-tagged strains (see Video S1 in the supplemental material) are shown using light microscopy, DIC (A) and epifluorescence (B, gray), to visualize live, attached *Giardia* trophozoites of the δ-giardin::GFP-tagged strain. Note the continuity of the ventral disc and the absence of δ-giardin in the bare area (ba), the central region of the ventral disc containing numerous vesicles and lacking the microtubule spiral array. (C) The MBP::GFP signal (green) colocalizes with δ-giardin as shown by immunostaining with anti-δ-giardin (red). (D to F) Morpholino knockdown of the median body protein in δ-giardin::GFP (green) trophozoites immunostained with anti-α-tubulin (red). (D) Unelectroporated trophozoites; (E) missense morpholino control; (F) anti-MBP morpholino. Knockdown of MBP results in an open conformation at the anterior end of the ventral disc (F, arrowheads). (G to I) Morpholino knockdown of MBP in the DAP17096::GFP strain, where GFP (green) marks the lateral crest structure. Anti-β-giardin immunostaining (red) is used to visualize the ventral disc. After treatment with the anti-MBP morpholino, trophozoites with the open ventral disc conformation (I, red) also had a discontinuous lateral crest (I, arrowhead) compared to the unelectroporated (G) or missense morpholino (H) trophozoites. DAPI (blue) stains the two nuclei (D to I). Bars = 2.5 μm.

strain to mark the ventral disc in live and fixed trophozoites (Fig. 3) and immunostained the MT cytoskeleton using TAT1 (5). MBP::GFP colocalizes with δ-giardin (Fig. 2). We saw no discernible differences in the median body presence or structure (33) after MBP knockdown. We did observe unique changes to the ventral disc structure, however (Fig. 3). Specifically, we observed that in ~20% of trophozoites the disc displayed an open or horseshoe conformation, as opposed to the typical circular overlapping shape. Over 50 percent of trophozoites did not show an obviously open disc conformation, yet the ventral disc appeared to have regions of less regular or evenly spaced microtubules and associated microribbons compared to unelectroporated controls.

The lateral crest surrounding the ventral disc is believed to be important for creating a seal that would enable suction-based attachment (16, 25). We recently identified 18 new DAPs, with 10 localizing specifically to the lateral crest region of the ventral disc (19). To determine if the knockdown of the median body protein that resulted in misshaped ventral discs would affect the structure and positioning of the lateral crest, we electroporated the anti-MBP morpholino into the DAP17096::GFP strain. DAP17096 is one of several ankyrin-repeat proteins localizing to the lateral crest (19), permitting us to assess lateral crest placement in trophozoites with the horseshoe disc phenotype. To visualize the ventral disc and more easily find cells with the horseshoe phenotype, trophozoites were also immunostained with an antibody to β-giardin (7). Forty-eight hours after the electroporation of the anti-MBP morpholino, we found that trophozoites with an open ventral disc did not have a properly formed lateral crest compared to missense morpholino or wild-type controls (Fig. 3). The lateral crest of these cells was open and followed the shape of the open disc, resulting in a horseshoe-shaped lateral crest.

Anti-MBP morpholino-treated trophozoites have reduced levels of attachment and aberrant surface contacts. To assess how defects in ventral disc structure affect attachment, we assayed

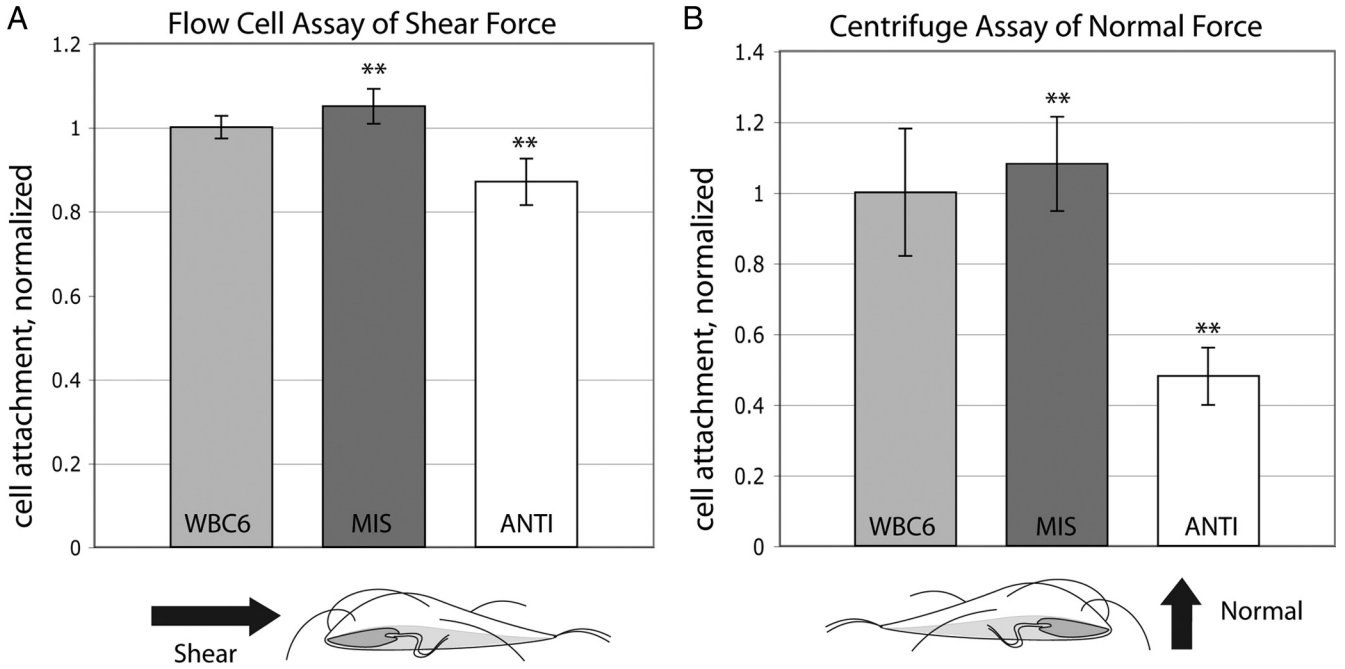

FIG 4 Anti-MBP morpholino-treated trophozoites have reduced levels of attachment in two live biophysical assays. Two biophysical assays measured either shear forces (A) or normal forces (B) of attachment in trophozoite populations 48 h after treatment with the anti-MBP morpholino (ANTI) compared to untreated wild-type (WBC6) cells or trophozoites treated with a missense morpholino (MIS). Double asterisks, significant ($P < 0.01$ by *t* test) decreases in attachment compared to missense morpholino-treated controls.

both normal and shear forces of attachment using previously described biophysical assays (20, 21). To assess shear forces in the anti-MBP morpholino-treated cells, trophozoites were challenged with shear stress using laminar flow. We observed a significant decrease (~15%) in the ability of anti-MBP morpholino-treated trophozoites to withstand shear forces compared to those treated with a missense morpholino or wild-type controls (Fig. 4). With respect to normal forces of attachment, we found that trophozoites treated with the anti-MBP morpholino also showed a significant (>50%) decrease in their ability to withstand normal forces compared to missense morpholino or wild-type controls (Fig. 4).

We found aberrant surface contacts using TIRFM and confocal live imaging of the anti-MBP morpholino-treated δ-giardin::GFP strain (which has a GFP-labeled ventral disc) stained with CellMask Orange to mark the plasma membrane (Fig. 5). Specifically, we observed that in trophozoites with the open disc conformation, the bare area extended throughout the opening toward the more anterior end of the cell, contiguous with the lateral crest. Surface contacts that characterize later stages of attachment following the skimming stage (25), such as the lateral crest seal, the lateral shield contacts, and a central bare area contact, were not present or aberrant in the morpholino-treated trophozoites (Fig. 5). Specifically, the late-stage bare area contacts were present in trophozoites with the open disc conformation, but the bare area contacts were misshapen (Fig. 5).

Three-dimensional live imaging of anti-MBP knockdowns indicates that the ventral disc is in a flattened conformation. Treatment of the δ-giardin::GFP strain with the anti-MBP morpholino not only resulted in an open disc conformation in the *xy* plane but also resulted in defects in the overall three-dimensional structure of the ventral disc. During late-stage attachment (e.g., lateral crest and lateral shield contacts), the ventral disc has a dome-shaped conformation (a height of about 2.8 μm at the most distal point from the surface, with an overall disc diameter of about 7.5 μm that does not change when the lateral crest seal is formed). The bare area contacting the surface characterizes the last stage of attachment. Using confocal live imaging of late-stage attached trophozoites, we found that that the ventral disc adopts a flattened, not a domed, conformation in attached trophozoites with the open disc phenotype, with an average height of about 0.7 μm and an average disc diameter of about 8.2 μm (Fig. 6).

DISCUSSION

Giardia attaches to the intestinal epithelium (or to inert surfaces) using an undefined suction-based mechanism (21), allowing parasites to colonize the small intestine to resist peristalsis. The unique and highly organized spiral MT array structure of the ventral disc is critical to virulence as it promotes attachment of *Giardia* to the intestinal epithelium (13). The ventral disc is composed of three main elements: (i) a domed right-handed spiral MT array nucleated by the caudal flagellar basal bodies, (ii) trilaminar microribbons that attach perpendicularly along the length of the MT spiral and extend into the cytoplasm, and (iii) cross-bridge structures that horizontally link the microribbons (7, 8, 15, 22–24). A bare area, central to the region where the disc MTs overlap (Fig. 1), contains numerous membrane-bound vacuoles. Additionally, the ventral disc is surrounded by the lateral crest, a fibrillar structure of unknown composition with proposed contractile functions (27). We have recently identified 18 novel DAPs, one of which is MBP, which conflicts with prior descriptions of this protein. We propose that the name "median body protein" be dropped in fa-

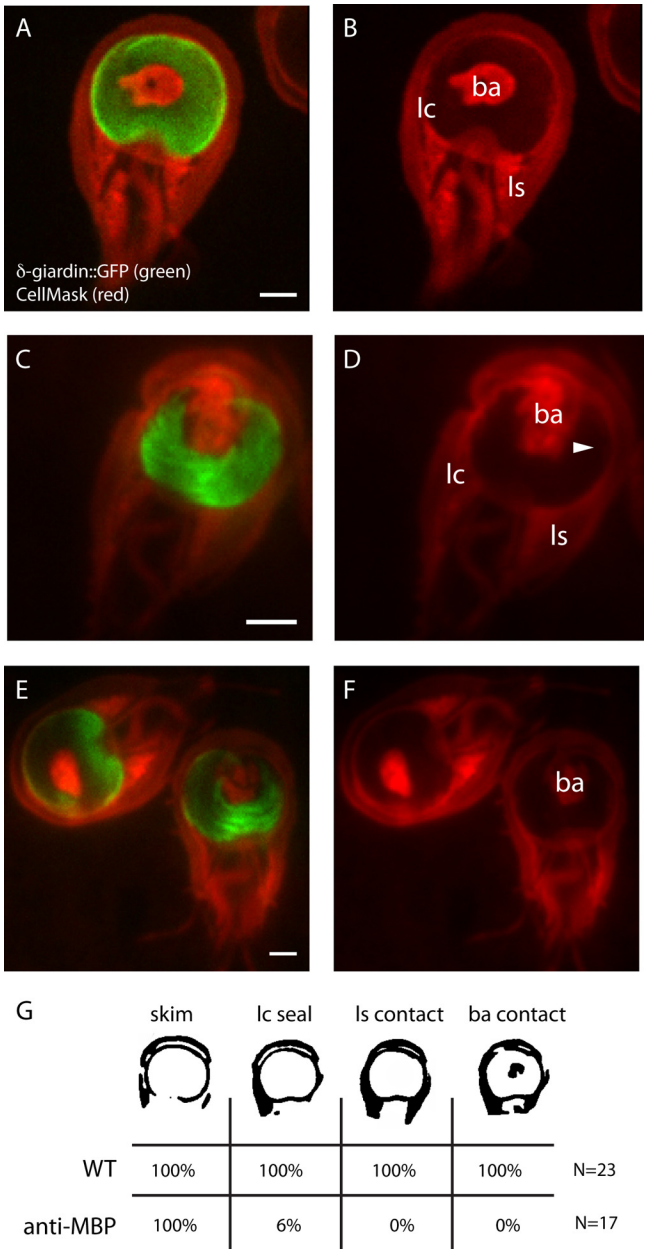

FIG 5 MBP knockdown results in aberrant surface contacts in trophozoites with an open ventral disc conformation. Live, attached trophozoites stained with CellMask (Invitrogen) to label the plasma membrane and imaged in three dimensions to show the surface contact points of the lateral crest (lc), the lateral shield (ls), and the bare area (ba). (A to F) Trophozoite surface contacts in the δ-giardin::GFP strain (green) after the electroporation of the anti-MBP morpholino in trophozoites with the wild-type closed (A and B) or the atypical open disc (C to F) conformations. Trophozoites were imaged using TIRFM after staining the membrane with CellMask (red). Note the open disc conformation in panel C and the aberrant and less intense bare area and lateral crest and lateral shield contacts in panel D compared to those in panel B. (E and F) Two adjacent trophozoites with both open and closed disc conformations. Anti-MBP trophozoites failed to progress to later attachment stages compared to wild type (summarized in panel G). Bars = 1 μm.

vor of the more descriptive name DAP16343, which indicates the GiardiaDB open reading frame identifier and that it is a DAP.

The median body protein is a structural component of the ventral disc during interphase. The 101-kDa coiled coil median body protein (29) was named on the basis of its initial immunolocalization to the median body of interphase trophozoites. Recently, however, we have identified MBP to be an abundant protein in the ventral disc proteome (19), and we have now used protein tagging approaches to show that the median body protein localizes primarily to the entire ventral disc structure (Fig. 2) and only secondarily to the median body. The difference in MBP localization between the two studies is likely a result of the different approaches used. In the earlier study, a polyclonal MBP antibody was used to immunolocalize MBP. The lack of MBP localization to the ventral disc may be a result of steric hindrance preventing access of both primary and secondary antibodies to MBP in the tightly packed disc structure; in fact, other disc-associated proteins, such as tubulin, are also known to be difficult to localize to the ventral disc by immunostaining (5). Furthermore, Marshall and Holberton used for their immunolocalizations detergent-extracted cytoskeletons that had been repeatedly washed rather than whole, fixed trophozoites (29). Thus, any association of the MBP with the ventral disc structure may have been disrupted in the particular preparation of cytoskeletons used for immunostaining (29). In addition to confirming the localization of MBP to the ventral disc, we have also shown that MBP is an essential structural component of the disc.

MBP is critical for maintaining a domed disc conformation during later stages of attachment. The ventral disc has been shown to be necessary for attachment of *Giardia* to different substrates (21), yet the role of specific disc conformational changes in attachment is less understood. Attachment, ventral disc conformational dynamics, and contacts of trophozoites with a glass substrate can be quantified using three-dimensional live imaging (11, 25). We have previously demonstrated that attachment of live trophozoites occurs within seconds as a stepwise process characterized by defined contacts of the trophozoite with an inert surface. The attachment process can be visualized using TIRFM (25). Four distinct stages of attachment include skimming, formation of a lateral crest seal at the disc perimeter, increased contact of the lateral shield region of the cell body, and lastly, increased contact of the bare area region central to the disc (see Fig. 1 and reference 25). During these stages of attachment, the microtubule-based structure of the ventral disc remains in a domed conformation; only the lateral crest and bare area regions contact the surface.

In the anti-MBP morpholino-treated trophozoites, conformational defects in the ventral disc and lateral crest may contribute to the observed lack of robust attachment. We observed notable localization of the MBP to the overlap zone of the ventral disc and saw that upon disruption of the disc using anti-MBP morpholinos, the overlap zone no longer formed (Fig. 3). The resulting open or horseshoe-shaped disc was no longer domed but rather adopted a flat conformation (Fig. 6). Thus, the MBP either directly or indirectly links the upper and lower regions of the ventral disc during disc biogenesis to promote the domed structure observed in live imaging of attached cells.

TIRFM live imaging showed that anti-MBP-treated cells also exhibited defects in surface contacts, and those with open disc conformations were unable to proceed through all stages of attachment (Fig. 5). In particular, the majority of cells with open

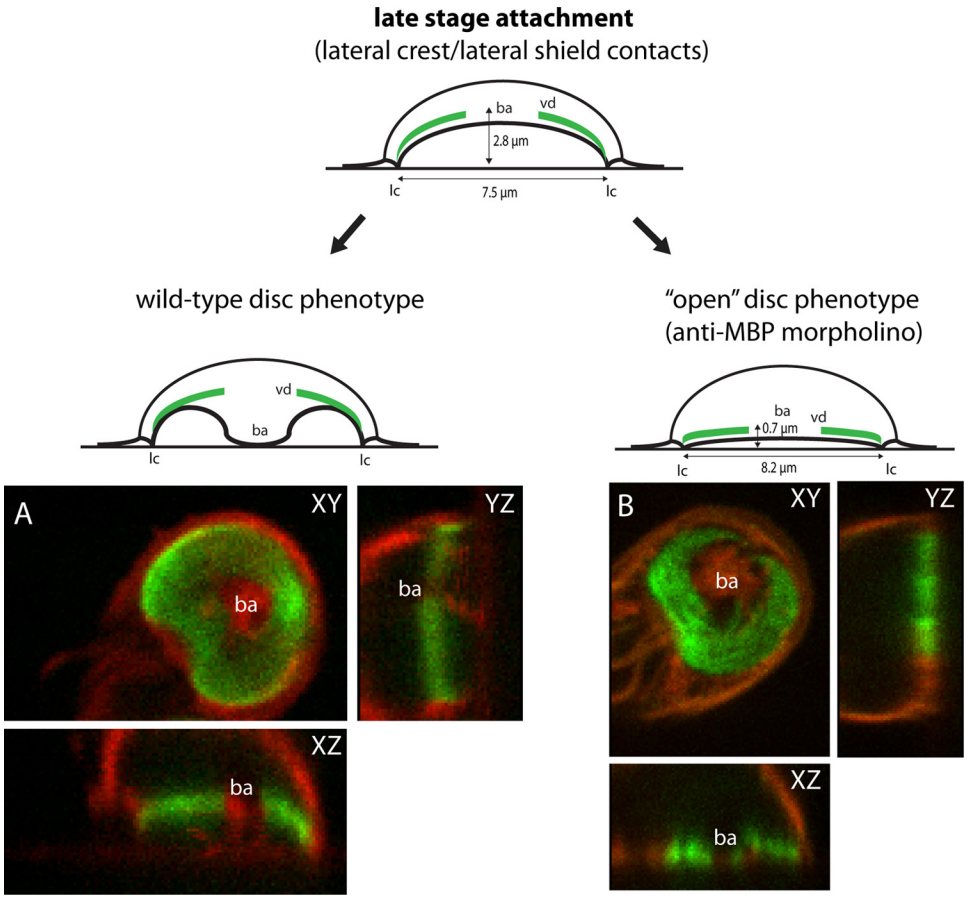

FIG 6 Trophozoites with an open ventral disc conformation also possess a flattened conformation in late stages of attachment. The typical closed and domed ventral disc conformation (green) of late-stage attached trophozoites is contrasted with the aberrant open and nondomed ventral disc conformation of anti-MBP morpholino-treated trophozoites. Ventral discs of the attached δ-giardin::GFP strain exhibit a domed ventral disc conformation (A) (see Video S2 in the supplemental material) as viewed with 3D live imaging (green, δ-giardin::GFP; red, CellMask). In contrast, anti-MBP-treated trophozoites with the open disc phenotype have a flat disc conformation that lacks concavity (B) (see Video S3 in the supplemental material). Measurements of disc height and width are based on 3D confocal imaging of the attached δ-giardin::GFP strain (see Materials and Methods) using the ventral disc (vd), bare area (ba), and lateral crest (lc) as cytological markers.

disc conformations had improper lateral crest or lateral shield contacts, and the bare area contacts were misshapen and continuous with the ventrolateral flange (Fig. 5). The seal formed by the lateral crest presumably enables or maintains a negative pressure differential underneath the disc during attachment (16, 25). The open and flattened ventral disc conformation in the anti-MBP morpholino-treated cells (Fig. 5 and 6) likely resulted in the lack of the negative pressure differential underneath the disc proposed to be responsible for disc-mediated suction (21).

We also used two biophysical assays of live populations of trophozoites to ascertain defects in resisting increased shear and normal forces (Fig. 4). Significant proportions of anti-MBP-treated trophozoites had attachment defects as measured by these assays (Fig. 4). Each assay challenges trophozoites with a different force; thus, significant differences between the two assays in terms of the numbers of trophozoites that remain attached are not unexpected. Taken together with the weaker and aberrant surface contacts observed in anti-MBP-treated trophozoites using TIRFM (Fig. 5 and 6), we contend that the defects in ventral disc conformation and lateral crest structure arising after depletion of MBP cause the observed decreases in attachment as quantified at the population level in the two biophysical attachment assays (Fig. 4). It is likely that *Giardia* attachment is not mediated by any single factor and that the requirement for a dome-shaped ventral disc with a complete lateral seal and proper surface contacts is greater when resisting normal forces than when resisting shear forces.

These observations support the idea that a domed conformation of the ventral disc is necessary for robust attachment of live cells. Suction-based forces could theoretically be generated directly via a conformational change of the ventral disc to a domed shape, resulting in a negative pressure differential relative to the outside medium. Alternatively, the ventral disc might retain its rigid, domed conformation and some other mechanism, such as an osmotic pressure-based mechanism of attachment in which the attachment force is generated by an osmotic pressure differential (20), could generate suction. A dome-shaped disc might also be required for proper lateral crest seal formation, which is an earlier stage in attachment (25).

Role of median body and MBP in ventral disc biogenesis. During cell division and cytokinesis, the eight flagella, median body, and ventral disc each undergo dramatic subcellular rearrangements prior to their partitioning into the daughter cells (31).

Two new daughter discs are assembled *de novo* on the dorsal side of the cell in telophase and are neither templated nor built from components of the parental disc. The parental disc is reorganized and disassembled after cell division (38) and also during encystation (17). Rapid assembly of the ventral disc would minimize the chances of the trophozoite being removed by peristalsis. Understanding how MBP is incorporated into the ventral disc during its assembly may inform our understanding of disc-mediated attachment.

Knockdown of MBP resulted in open, flat ventral discs, suggesting that MBP links the overlapping regions of the ventral disc spiral and is required for proper assembly of the three-dimensional architecture of the disc. Most of the ventral disc is assembled properly following MBP knockdown, yet the overlap zone remains discontinuous. With respect to the timing of events during disc biogenesis, this implies that assembly of most of the ventral disc occurs before it undergoes conformational changes to become an overlapping spiral with an overall domed shape. Trophozoites that exhibited an open overlap zone after MBP knockdown also had a discontinuous lateral crest, as visualized using DAP17096::GFP. Based on the discontinuity of the lateral crest in these anti-MBP morpholino-treated cells, we propose that the lateral crest is assembled after assembly of the main MT-based structures of the ventral disc.

Why does the MBP occasionally localize to the median body? It has been suggested that the median body is a reservoir of MTs that are somehow recruited to new daughter discs during cell division (4, 14). In addition to DAP16343, several other lateral crest- and disc-associated protein components are known to assemble on median body MTs (7), supporting the idea that ventral disc components assemble on median body microtubules prior to dorsal disc biogenesis.

Concluding remarks. Site recognition, flagellar motility, and specific disc conformations each likely contribute to *in vivo* attachment. Drugs affecting ventral disc structure, disc biogenesis, or disc conformational dynamics may directly or indirectly decrease trophozoite attachment in the host and thus limit the initiation or extent of infection. Previous technical limitations have made studying the role of the ventral disc in attachment difficult at the molecular and cellular levels (9, 13); however, recently developed molecular tools to study protein function (6) permit detailed analyses of newly described ventral disc components (19). Understanding the active role of ventral disc conformational dynamics or the passive role of the ventral disc in maintaining a negative pressure differential is critical toward developing new classes of anti-*Giardia* compounds.

ACKNOWLEDGMENTS

We thank Kari Hagen for valuable editorial assistance and Susan House (Dawson lab), Cindi Schwartz (CU—Boulder), and Joel Mancuso (UC Berkeley) for microscopy training and expertise. The TAT1 antibody was a kind gift from Keith Gull (Oxford University). The β-giardin antibody was a kind gift from Heidi Elmendorf (Georgetown University).

S.C.D. and D.J.W. conceived and designed the experiments. D.J.W. performed the experiments. D.J.W. and S.C.D. analyzed the data. D.J.W. and S.C.D. wrote the paper.

REFERENCES

1. **Adam RD.** 2001. Biology of *Giardia lamblia*. Clin. Microbiol. Rev. **14**: 447–475.
2. **Axelrod D.** 2001. Total internal reflection fluorescence microscopy in cell biology. Traffic **2**:764–774.
3. **Barat LM, Bloland PB.** 1997. Drug resistance among malaria and other parasites. Infect. Dis. Clin. North Am. **11**:969–987.
4. **Brugerolle G.** 1975. Contribution à l' étude cytologique et phylétique des diplozoaires (Zoomastigophorea, Diplozoa, Dangeard 1910). V. Nouvelle interpretation de l'organisation cellulaire de Giardie. Protistologica **11**: 99–109.
5. **Campanati L, et al.** 2003. Tubulin diversity in trophozoites of *Giardia lamblia*. Histochem. Cell Biol. **119**:323–331.
6. **Carpenter ML, Cande WZ.** 2009. Using morpholinos for gene knockdown in *Giardia intestinalis*. Eukaryot. Cell **8**:916–919.
7. **Crossley R, Holberton DV.** 1985. Assembly of 2.5 nm filaments from giardin, a protein associated with cytoskeletal microtubules in *Giardia*. J. Cell Sci. **78**:205–231.
8. **Crossley R, Holberton DV.** 1983. Characterization of proteins from the cytoskeleton of *Giardia lamblia*. J. Cell Sci. **59**:81–103.
9. **Davis-Hayman SR, Nash TE.** 2002. Genetic manipulation of *Giardia lamblia*. Mol. Biochem. Parasitol. **122**:1–7.
10. **Dawson SC.** 2010. An insider's guide to the microtubule cytoskeleton of *Giardia*. Cell. Microbiol. **12**:588–598.
11. **Dawson SC, House SA.** 2010. Imaging and analysis of the microtubule cytoskeleton in *Giardia*. Methods Cell Biol. **97**:307–339.
12. **Dawson SC, et al.** 2007. Kinesin-13 regulates flagellar, interphase, and mitotic microtubule dynamics in *Giardia intestinalis*. Eukaryot. Cell **6**:2354–2364.
13. **Elmendorf HG, Dawson SC, McCaffery JM.** 2003. The cytoskeleton of *Giardia lamblia*. Int. J. Parasitol. **33**:3–28.
14. **Feely D, Holberton DV, Erlandsen SL.** 1990. The biology of *Giardia*, p 11–50. *In* Meyer EA (ed), Giardiasis, vol 3. Elsevier, Amsterdam, The Netherlands.
15. **Feely DE, Schollmeyer JV, Erlandsen SL.** 1982. *Giardia* spp.: distribution of contractile proteins in the attachment organelle. Exp. Parasitol. **53**:145–154.
16. **Friend DS.** 1966. The fine structure of *Giardia muris*. J. Cell Biol. **29**:317–332.
17. **Gillin FD, Reiner DS, McCaffery JM.** 1996. Cell biology of the primitive eukaryote *Giardia lamblia*. Annu. Rev. Microbiol. **50**:679–705.
18. **Gourguechon S, Cande WZ.** 2011. Rapid tagging and integration of genes in *Giardia intestinalis*. Eukaryot. Cell **10**:142–145.
19. **Hagen KD, et al.** 2011. Novel structural components of the ventral disc and lateral crest in *Giardia intestinalis*. PLoS Negl. Trop. Dis. **5**:e1442.
20. **Hansen WR, Fletcher DA.** 2008. Tonic shock induces detachment of *Giardia lamblia*. PLoS Negl. Trop. Dis. **2**:e169.
21. **Hansen WR, Tulyathan O, Dawson SC, Cande WZ, Fletcher DA.** 2006. *Giardia lamblia* attachment force is insensitive to surface treatments. Eukaryot. Cell **5**:781–783.
22. **Holberton DV.** 1981. Arrangement of subunits in microribbons from *Giardia*. J. Cell Sci. **47**:167–185.
23. **Holberton DV.** 1973. Fine structure of the ventral disk apparatus and the mechanism of attachment in the flagellate *Giardia muris*. J. Cell Sci. **13**: 11–41.
24. **Holberton DV, Ward AP.** 1981. Isolation of the cytoskeleton from *Giardia*. Tubulin and a low-molecular-weight protein associated with microribbon structures. J. Cell Sci. **47**:139–166.
25. **House SA, Richter DJ, Pham JK, Dawson SC.** 2011. *Giardia* flagellar motility is not directly required to maintain attachment to surfaces. PLoS Pathog. **7**:e1002167.
26. **Keister DB.** 1983. Axenic culture of *Giardia lamblia* in TYI-S-33 medium supplemented with bile. Trans. R. Soc. Trop. Med. Hyg. **77**:487–488.
27. **Kulda J, Nohynkova E.** 1995. *Giardia* in humans and animals, p 225–423. *In* Kreier JP (ed), Parasitic protozoa, vol 10. Academic Press, Inc., San Diego, CA.
28. **Land KM, Johnson PJ.** 1999. Molecular basis of metronidazole resistance in pathogenic bacteria and protozoa. Drug Resist Updat. **2**:289–294.
29. **Marshall J, Holberton DV.** 1993. Sequence and structure of a new coiled coil protein from a microtubule bundle in *Giardia*. J. Mol. Biol. **231**:521–530.
30. **Morrison HG, et al.** 2007. Genomic minimalism in the early diverging intestinal parasite *Giardia lamblia*. Science **317**:1921–1926.
31. **Nohynkova E, Tumova P, Kulda J.** 2006. Cell division of *Giardia intestinalis*: flagellar developmental cycle involves transformation and exchange of flagella between mastigonts of a diplomonad cell. Eukaryot. Cell **5**:753–761.
32. **Paredez AR, et al.** 2011. An actin cytoskeleton with evolutionarily con-

served functions in the absence of canonical actin-binding proteins. Proc. Natl. Acad. Sci. U. S. A. **108**:6151–6156.
33. **Piva B, Benchimol M.** 2004. The median body of *Giardia lamblia*: an ultrastructural study. Biol. Cell **96**:735–746.
34. **Sagolla MS, Dawson SC, Mancuso JJ, Cande WZ.** 2006. Three-dimensional analysis of mitosis and cytokinesis in the binucleate parasite *Giardia intestinalis*. J. Cell Sci. **119**:4889–4900.
35. **Savioli L, Smith H, Thompson A.** 2006. *Giardia* and *Cryptosporidium* join the 'Neglected Diseases Initiative.' Trends Parasitol. **22**:203–208.
36. **Sullivan KF, Kay SA.** 1999. Green fluorescent proteins. Academic Press, San Diego, CA.
37. **Troeger H, et al.** 2007. Effect of chronic *Giardia lamblia* infection on epithelial transport and barrier function in human duodenum. Gut **56**:328–335.
38. **Tumova P, Kulda J, Nohynkova E.** 2007. Cell division of *Giardia intestinalis*: assembly and disassembly of the adhesive disc, and the cytokinesis. Cell Motil. Cytoskeleton **64**:288–298.
39. **Upcroft J, Samarawickrema N, Brown D, Upcroft P.** 1996. Mechanisms of metronidazole resistance in *Giardia and Entamoeba*, p 47. Abstr. 36th Intersci. Conf. Antimicrob. Agents Chemother. American Society for Microbiology, Washington, DC.
40. **Zeng X, et al.** 1999. Slk19p is a centromere protein that functions to stabilize mitotic spindles. J. Cell Biol. **146**:415–425.